Sediment texture, erodibility, and composition in the Northern Gulf of Mexico and their potential impacts on hypoxia formation

Rangley Mickey · Kehui Xu · Susan Libes · Jenna Hill

Abstract A region of hypoxic waters has formed annually over the past several decades in the northern Gulf of Mexico. This has motivated the studies of mechanisms controlling the development of hypoxia. Both field and laboratory approaches were used to examine sediment texture, erodibility, and composition. Sediment texture analyses show that grain size relates to the proximity to the Mississippi and Atchafalaya river deltas and to the remnants of shifts in the Mississippi and Atchafalaya deltaic lobes. Temporal variability in erodibility relates to seasonal weather patterns, with more energetic wave conditions in winter and spring setting up an active bottom layer that increases erodibility, compared to quiescent summers that allow for seabed consolidation. The amount of eroded material is fairly low until shear stress levels in the bottom boundary layer exceed 0.4 Pa. An organically enriched fluff layer was found at the sediment–water interface, which is highly erodible under low shear stress levels. Eroded volatile suspended solids (a proxy for organic material) vs. increasing levels of shear stress revealed a distinct pattern at all sample areas; higher concentrations of organic material were eroded at the lowest (0.01 Pa) and highest (0.6 Pa) applied shear stresses, and there was a higher ratio of the volatile to total suspended solids at 0.01 Pa. Based on erodibility experiments and modeling data analysis, the low shear stress levels during the quiescent periods in summer were sometimes high enough to resuspend this fluff layer, but not underlying sediment, thereby potentially facilitating the development of bottom water hypoxia.

R. Mickey · S. Libes · J. Hill
School of Coastal Marine System Science, Coastal Carolina University, P.O. Box 261954, Conway, SC 29526, USA

K. Xu
Department of Oceanography and Coastal Sciences, Louisiana State University, Baton Rouge, LA 70803, USA

K. Xu
Coastal Studies Institute, Louisiana State University, Baton Rouge, LA 70803, USA

R. Mickey (✉)
USGS, 600 4th Street South, St Petersburg, FL 33701, USA
e-mail: rmickey@usgs.gov

1 Introduction

One of the largest hypoxic (dissolved oxygen<2 mg/L) events occurs annually in the northern Gulf of Mexico (nGOM) during the warm months of the year (Rabalais et al. 2007). The seasonal development of hypoxia in the nGOM is thought to be the result from a combination of eutrophication that arises from excessive nutrient loading from the Mississippi River watershed in the spring and temperature- and salinity-driven water column stratification during the summer (Rabalais et al. 2007). The Mississippi River watershed is the largest in the USA, draining nearly 41 % of the nation's continental landmass into the nGOM (Environmental Protection Agency). The Mississippi River system has two main outlets to the gulf: the Mississippi and Atchafalaya Rivers. During the past several decades, both rivers have delivered ~70 and ~30 %, respectively, of the total discharge into the nGOM (Meade and Moody 2010). The input of nutrients from these two rivers causes high productivity in the nGOM during the spring months, thereby increasing the amount of autochthonous detritus introduced into the lower water column and underlying sediment. This leads to

increased aerobic respiration by heterotrophic bacteria (Rabalais et al. 2007). Bottom water hypoxia is most prevalent during the late spring and summer months due to strong stratification of the water column, which decreases the amount of mixing and slows down reoxygenation in the lower water column (below the major pycnocline). The spatial extent of hypoxia increases dramatically such that within weeks, the maximum areal extent ranges from 8,000 to 20,000 km^2. From 1985 to 2007, for example, the annual average extent of the hypoxic zone has been approximately 13,000 km^2 (Rabalais et al. 2007). Studies demonstrate that during this time period, the annual extent of the hypoxic zone exhibited a positive linear correlation with riverine nitrogen input (Turner et al. 2006, 2008). This has been attributed to an increase in phytoplankton growth above normal abundances (Rabalais et al. 2007). When these algal bloom die, or are consumed by zooplankton and turned into fecal matter, the detrital material sinks through the water column and is then respired by heterotrophic bacteria (Dagg et al. 2008). Depending on sinking rates and the depth of the water column, some detritus can reach the surface of the seabed.

When productivity increases due to large nutrient inputs, organic material (OM) and some aggregated fine-grained minerals are deposited on the sediment surface, forming a "fluff layer" of fine loose material. The amount and composition of material setting through the lower water column and depositing on the sediment surface are dependent on processes acting on both organic and inorganic sinking particles, including aggregation–disaggregation, sorption–desorption, photo-oxidation, and mineralization (Mckee et al. 2004). The fluff layer that settles on the surficial sediment is comprised of unconsolidated, easily resuspended, and low-density materials (Wainright and Hopkinson 1997). Rowe et al. (2002) have observed that the sediment–water interface is a major site of enhanced bacterial concentration and presumably of aerobic respiration rates. The presence of this fluff layer at the sediment–water interface may be a significant source of labile OM that could influence hypoxic regimes in the nGOM (Gardner et al. 2009).

Organic sediments have the potential to influence development of hypoxia as they can support biological and chemical uptake of oxygen. This uptake is referred to be sediment oxygen demand (SOD). Evidence for the extent of this influence ranges from studies suggesting SOD contributes up to 73 % of the total oxygen consumption in hypoxic bottom waters (Quinones-Rivera et al. 2007) to others that indicate SOD contributes less than 20 % of the total below-pycnocline respiration (Murrell and Lehrter 2010).

Prolonged nutrient loading into the nGOM has resulted in increased accumulations of OM in the surface sediments (Turner et al. 2008). These increases are attributed, at least in part, to incomplete respiration, leading to an increasing reservoir of sedimentary OM in seabed and hence an increasing SOD (Turner et al. 2008). As a result, a larger aerial extent of hypoxia can arise without a simultaneous increase in seasonal riverine nutrient loading. This represents an alternate state for the nGOM that will be difficult to recover from, even with decreased nutrient loading, as remineralization of nutrients during the respiration of the buried OM will continue to support algal blooms, resupplying detrital OM and SOD back to the seabed surface (Turner et al. 2008). On the other hand, Turner et al. (2008) have reported that hypoxia could be reaching its geomorphological limit (25,000 km^2) due to physical constraints associated with the geometry of the northern Louisiana-Texas (LATEX) continental shelf. Grant et al. (1991) have suggested that muddy sediments, like those in the nGOM, may be important in terms of biological activity due to fine sediments having increased grain surface area, organic content, and bacterial biomass, which may enhance metabolic activity per unit seabed surface area. Their study of benthic oxygen consumption rates on the eastern Canadian continental shelf indicates significantly higher SOD in areas with fine (muddy) sediments compared to areas with coarser (sandy) sediments (Grant et al. 1991); mean benthic SOD rate was observed to be 2.7 times greater in finer grained sediments compared to coarser, indicating that grain size can play an important role in carbon consumption and SOD rates.

Physical processes, such as waves, tides, and currents, can also play a key role in sediment resuspension and associated SOD dynamics. These physical processes are important as they affect the extent to which the sedimentary particles are in contact with oxygenated seawater, nutrients, and microbes. Studies modeling the relationships between frequencies of resuspension events and mineralization indicate that as resuspension events increase in frequency, remineralization increases in the water column and decreases in the underlying surficial and deep sediments (Wainright and Hopkinson 1997). During the summer, resuspension events have the potential to greatly influence respiration rates at the sediment–water interface, leading to higher SOD rates (Wainright and Hopkinson 1997).

The presence of a fluff layer atop the sediment surface has been documented in areas around the world, and many studies have shown that this fluff layer is erodible at shear stresses between 0.01 and 0.05 Pa in shelf environments. In the southern Baltic Sea, for instance, Emeis et al. (2002) found the presence of an organically enriched fluffy layer of material covering the sandy nearshore sediments and were able to sample this layer by using divers to siphon it off the seabed surface. They found that the fluff material was enriched with OM but not significantly richer than OM in the water column (Emeis et al. 2002). Another study in the Baltic Sea by Christainsen et al. (2002) used a LABEREX chamber to measure threshold velocity for resuspension and found that threshold was around 0.02 Pa for the suspension of organically enriched fluff material atop the seabed surface.

Dickhudt et al. (2009) used a Gust Erosion Microcosm System (GEMS) in the York River estuary and found that material eroded at lower shear stress levels (0.05 Pa) was enriched with OM relative to material eroded at high shear stress levels. Maa et al. (1998) used the a Sea Carousel to study sediment resuspension in Baltimore Harbor and found that the measured critical bed shear stress strongly depends on the presence of a fluff layer; they also demonstrated that in some areas, fluff layer can be resuspended at very low shear stresses (0.01 Pa). Milligan and Law (2013) used the GEMS system to investigate environmental contaminants at the sediment–water interface in Novia Scotia and New Brunswick; they also found the fluff layer to be organically enriched and easily eroded at very low shear stress levels (0.01 Pa). All of the above studies have used various flumes, microcosms, and devices to study the fluff layer that has a critical shear stress much smaller than that of the underlying sediments, typically by an order of magnitude. Only a couple have examined the composition of the material eroded under very low levels of shear stress, which are indicative of the organically enriched fluff layer (Dickhudt et al. 2009; Emeis et al. 2002; Christainsen et al. 2002; Milligan and Law 2013).

During the past decade, several studies have quantified the texture of sediments in the nGOM (Buczkowski et al. 2006; gulfatlas.noaa.gov), especially in sediments from the hypoxic zone (Briggs et al. 2009), but very few have tried to analyze the fluff layer (Gardner et al. 2009). Rowe et al. (2002) identified the sediment–water interface as an important site of microbial respiration but did not study the fluff layer located at this interface in the nGOM. Murrell and Lehrter (2010) observed the presence of fluff layer when deploying benthic chambers and collecting sediment cores to estimate SOD rates in the hypoxic zone but gave no indication on the composition of this layer or its importance in influencing hypoxic regimes. This lack of SOD and OM studies on fluff layers was probably due to the challenge of collecting cores with an undisturbed sediment–water interface and subsampling the thin and mobile fluff layers as it is usually only a few to tens of millimeters thick. In many nGOM hypoxia studies along the 20-m isobaths, Conductivity, Temperature, and Depth (CTD) rosettes have been used to collect profiling data (e.g., temperature, salinity, and chlorophyll) from sea surface to about 1 m above sea bed, but the bottom boundary layer from seabed surface to 1 m above seabed has been *understudied* for a long period of time.

Recently, Gardner et al. (2009) designed a new HYPOX corer which allows for the retrieval of individual sediment cores with a relatively intact fluff layer at the sediment–water interface for the studies of chemical, physical, and biological mechanisms occurring at this interface. Xu et al. (2014) collected 106 sediment cores using the HYPOX and other coring devices on the LATEX shelf during five cruises in 2010 and 2011 and used a GEMS system to measure seabed erodibility before and after the 2011 Mississippi River flood; erodibility

generally refers to how easily material from the seabed surface may be eroded and resuspended into the water column under different levels of shear stress applied to the sediment surface. This study shows that with newly developed tools, the extraction of sediment cores with undisturbed fluff layers can be achieved, allowing for more refined studies of the fluff layer composition and erodibility in laboratory settings.

2 Objectives

In this study, sediment texture, erodibility, and composition are investigated to understand how sediment resuspension and fluff layer may impact the development of hypoxia in the nGOM. The studies of Xu et al. (2014) were focused on spatial variation of erodibility, x-radiograph, flood deposit thickness, and bioturbation, and their data were collected in five cruises in 2010 and 2011. In contrast, this study is focused on surficial grain size, temporal variation of erodibility along the 20-m isobath (the center of hypoxic water), and volatile suspended solids (proxy for OM), and the data were collected in five cruises in 2011 and 2012. Three objectives of this study are (1) to examine surficial sediment grain size variations at multiple stations across the LATEX shelf and determine both spatial and temporal variability, (2) to measure sediment erodibility and determine the amount of total suspended solids (TSS) eroded from sediment cores that were collected from the 20 m isobath in the nGOM hypoxic region; and (3) to measure the amount of volatile suspended solids (VSS) suspended when multiple levels of shear stress are applied since VSS could serve as a proxy for respirable OM reintroduced into the lower water column where hypoxia is prevalent.

The results from erodibility experiments and grain size analyses conducted during this study will provide insight into the physical conditions occurring at the sediment–water interface; these insights may aid future studies that analyze the influence of physical conditions on the biogeochemical cycles that contribute to the formation and maintenance of bottom hypoxic waters. With enhanced knowledge of these physical and biogeochemical interactions, more advanced 3-D modeling systems can be developed that would be able to accurately hindcast, nowcast, and forecast hypoxic events by coupling the physical model conditions with those of the biogeochemical models.

3 Materials and methods

3.1 Field cruises and core collections

Sediment sampling was carried out across the nGOM hypoxic zone on five research cruises during April 25–29, 2011,

August 3–8, 2011 (defined as early August 2011) and August 16–20, 2011 (middle August 2011), April 25–29, 2012, and August 7–11, 2012 (Table 1). Samples were collected at four stations across the nGOM: AB5 (defined as eastern hypoxic zone), 10B (middle hypoxic zone), 08C (western hypoxic zone), and Atch (south of Atchafalaya Bay) (Fig. 1). These stations were chosen based on their position across the LATEX shelf and proximity to areas of observed hypoxia. In early August 2011, surficial sediment samples were collected at 26 stations (NSF RAPID cruise) across the LATEX shelf (Fig. 1).

Two types of gravity corers were used to collect sediment samples, the HYPOX corer (Gardner et al. 2009) and a multi-corer (Table 1). Three sediment cores were collected within a 24-h period at each station for the cruises in 2011 and five cores within a 24-h period at each station for cruises in 2012. For 2012, erodibility experiments were conducted twice at each station for more replicates (Table 1). Of the three sediment cores collected in 2011 at each station, one core was used for sediment grain size sampling and the other two were stabilized for immediate setup of erodibility experiments using GEMS. These cores were fitted with a plastic plunger to maintain the sediment–water interface 10 cm from the top of the core and sealed at the bottom. The cores were then sealed on the bottom using the appropriate plugs and caps to prevent loss of water during transport from the deck to the ship's laboratory. Care was taken during transport to minimize disturbance of the fluff layer at the sediment surface.

3.2 Grain size analysis

The sediment core for grain size analysis was subsampled using a 12-cm-long modified syringe with a 2.5-cm diameter. These cores were then extruded and divided into 1-cm-thick slices. They were bagged, labeled, and frozen, and grain size analyses were performed using a Beckman-Coulter Laser Diffraction Particle Size Analyzer (model LS 13 320) on a 0.5-g subsample from each 1-cm slice. The sediment was placed into a vial with deionized water, shaken vigorously for 10 min to disaggregate the samples, and then poured into the analyzer. Neither organic matter nor carbonate was removed during this analysis. The analyzer can detect particles ranging from 0.02 to 2,000 μm in diameter. Down core grain size distribution was assessed from a total of 176 1-cm slices collected at four sites in April and August of 2011 and 2012. To characterize spatial variation in particle size distributions of surficial sediment (0–1 cm), 27 samples were analyzed from cores collected on the NSF RAPID cruise in early August 2011 as well, following the same method described above.

3.3 Erodibility experiments

The dual-core GEMS was used to measure sediment erodibility at the sampling stations. This system was developed by Gust and Muller (1997) and has been used in various environments of multiple studies, such as those listed in Section 1. This system includes a computer, a power control box, two turbidimeters, a pump controller, two rotating motors, two erosional heads, two sediment chambers, source water, collection bottles, and a suction filtration system (see detailed setup in Lo et al. (2014) and a picture in Xu et al. (2014)). There were a total of seven shear stress levels (τ_c) applied in succession to the sediment cores: 0.01, 0.05, 0.1, 0.2, 0.3, 0.45, and 0.6 Pa, respectively. Turbidity (in nephelometric turbidity units (NTU)) was measured throughout the entire experiment using two turbiditimeters, and the results were plotted with rotational speeds (in revolutions per minute (RPM)) (see Fig. 10) of the erosion motor heads. Seawater was collected at each site in 2011 from the sea surface and in 2012 from 1 m above the seabed using a CTD rosette and used as source water for the erodibility experiments. Each shear stress was applied for 20 min during the experiment, and the resulting sediment slurry was collected for analysis. The volume of the slurry was measured and filtered using a vacuum filtration system to collect the resuspended solids, on a pre-weighed 142-mm-diameter binder-free borosilicate glass fiber filter with a nominal pore size of 0.7 μm. The filtered solids were dried and weighed to determine the mass of TSS. In this study, the unit of TSS is milligrams per liter, which is milligram of suspended solids per liter of sediment slurry at

Table 1 Project names, dates, vessels, and sampling method for each research cruise on which samples were collected, also the number of stations visited on each cruise and the number of sediment cores collected on each cruise

Project	Month/year	Research vessel	Coring device	Stations	Cores for gust	Cores for grain size	Total cores collected
NOAA NGOMEX (MCH 17)	April 2011	Pelican	*Hypox*	4	8	4	12
NSF RAPID	Early August 2011	Cape Hatteras	Multi-core	28	6	27	56
NOAA NGOMEX (MCH 19)	Mid-August 2011	Pelican	*Hypox*	4	8	4	12
NOAA NGOMEX (MCH 20)	April 2012	Pelican	*Hypox*	4	16	4	20
NOAA NGOMEX (MCH 21)	August 2012	Pelican	*Hypox*	4	16	4	20

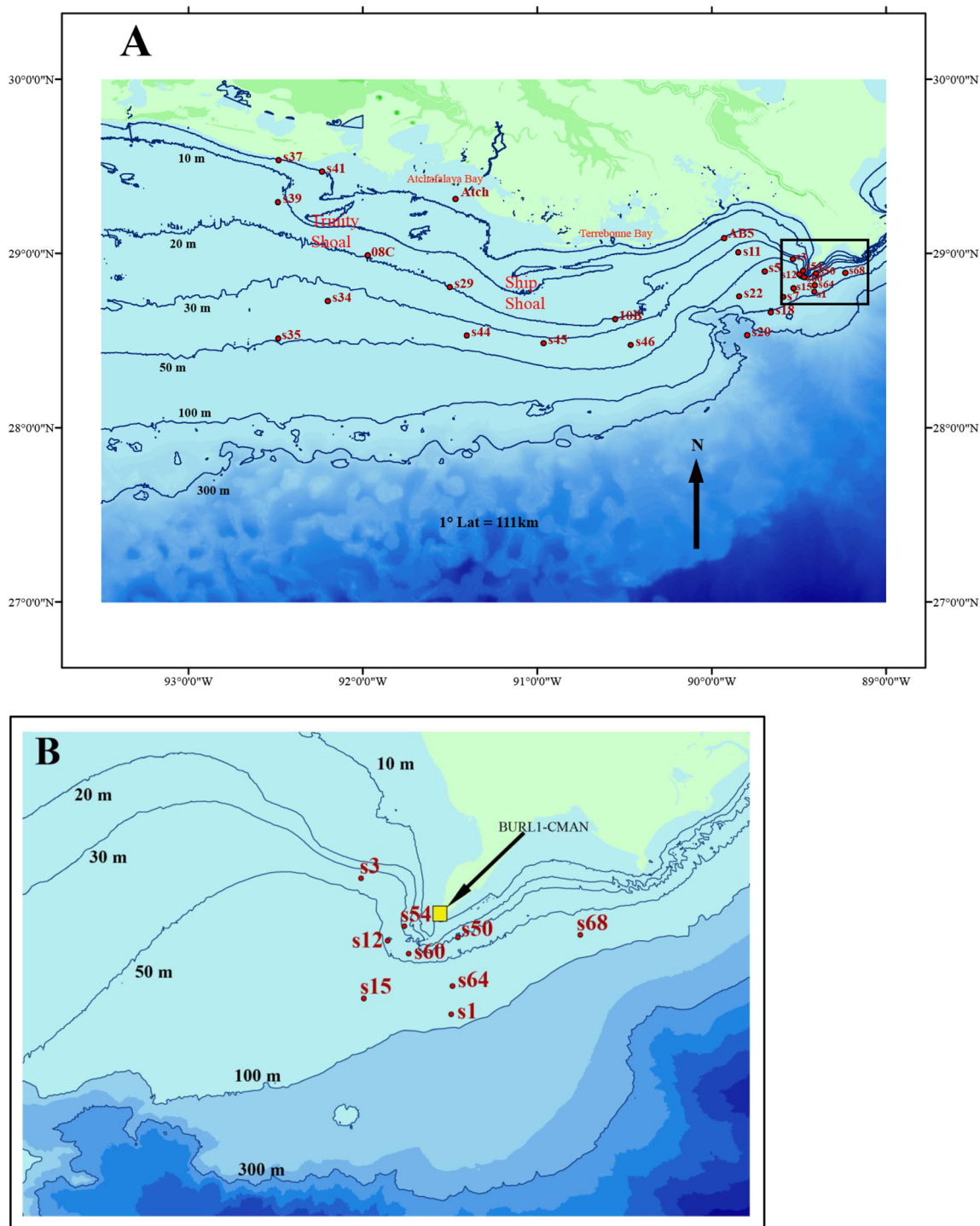*MCH* Mechanisms Controlling Hypoxia Research Group

Fig. 1 **a** Map of sampling locations, indicated by station labels, across the northern Gulf of Mexico. All sites were used in spatial variability analysis; only AB5, 10B, 08C, and Atch were used in temporal variability analysis. **b** An expanded version of the area bounded by the *box* in (**a**)

highlighting the southwest pass of the Mississippi River. *Yellow square* near Mississippi Southwest Pass represents the BURL1C-MAN weather station

each time step. The TSS and turbidity results were used to construct erodibility profiles following the methods of Sanford and Maa ([2001](#)) and the calculations provided by Dickhudt et al. ([2009](#)). Some additional erodibility experimental data collected in August of 2010 by Xu et al. ([2014](#))

were also analyzed in this study for the comparison of erodibility profiles at these four stations. The dried filtered sediments were ignited and the loss in weight was used to determine the amount of VSS, in milligrams per liter. The ignition was performed in a muffle furnace by combusting at 500 °C
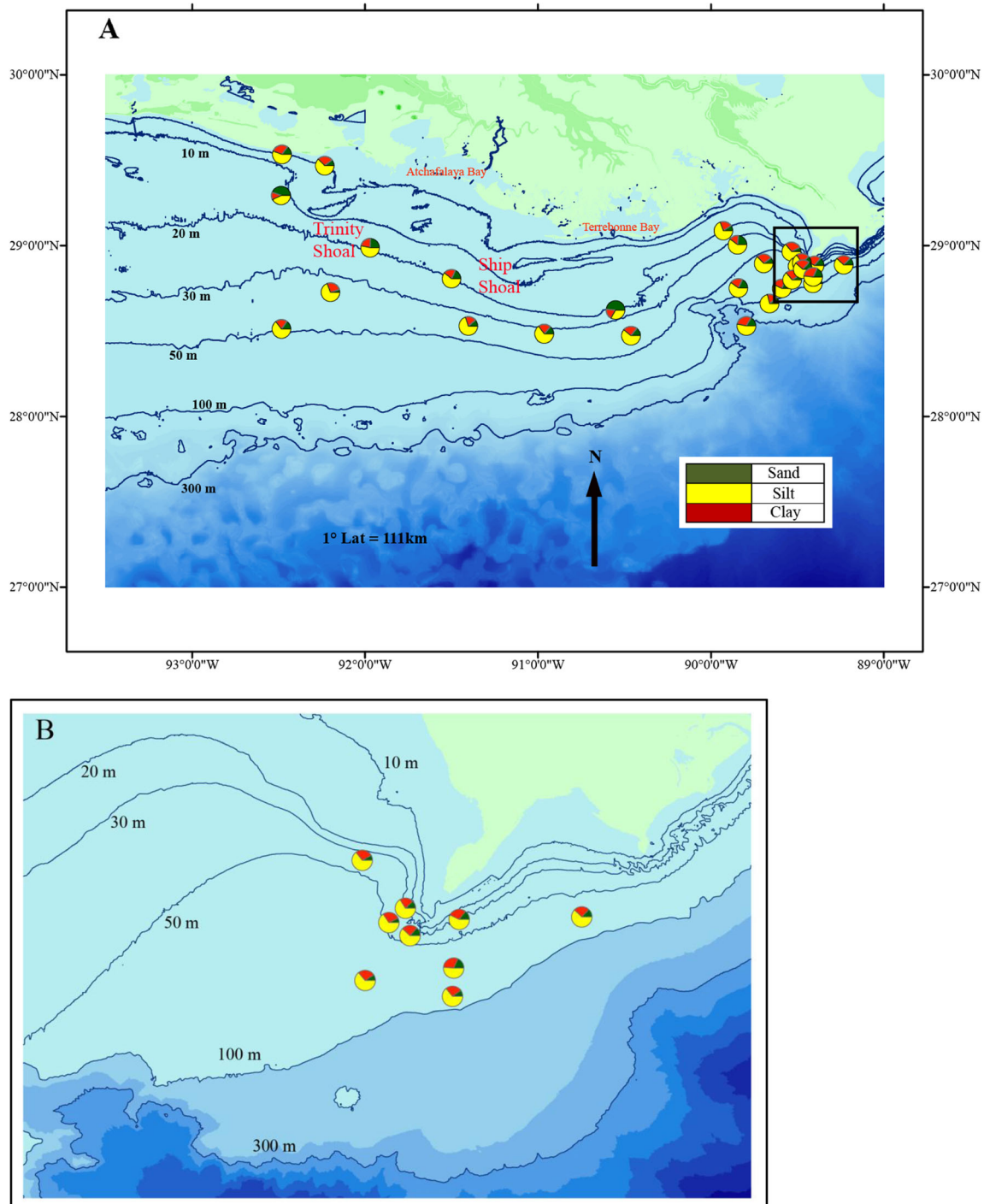
Fig. 2 **a** Plot of pie charts representing percentages of three sediment types: sand (*green*), silt (*yellow*), clay (*red*). **b** An expanded version of the area bounded by the box in (**a**) highlighting the mouth of the Southwest Pass of the Mississippi River

for about 4 h. The VSS analysis was performed only on samples from the April 2011, April 2012, and August 2012 cruises; time constraints immediately after the NSF RAPID and August 2011 cruise did not permit VSS analysis. The VSS in the resuspended materials collected during the erodibility experiments could have been derived from either the *source water* or the *resuspended sediments* in cores. Unfortunately,

source water TSS concentration was only measured in 2012 and not in 2011. To account for any background VSS in 2011, we subtracted the lowest measured VSS concentration during the experiment (usually around 0.2 Pa time step) from each VSS concentration at each applied shear stress; this conservative calculation should eliminate any background VSS from source water collected in

Table 2 Stations sampled during early August 2011 for the study of spatial variability in surficial grain size (Fig. 1)

Station ID	Longitude	Latitude	Depth	Mean	SD	Skew	Kurt	D10	D25	D50	D75	D90	% Clay	% Silt	% Sand
S1	−89.41	28.78	88.90	6.721	2.037	−0.034	1.195	3.985	5.527	6.737	7.951	9.350	23.97	66.06	9.968
S3	−89.53	28.96	37.30	6.876	1.903	−0.050	1.199	4.354	5.780	6.918	8.036	9.292	25.35	66.88	7.776
S5	−89.70	28.90	56.10	6.725	2.067	−0.083	1.264	3.822	5.591	6.795	7.956	9.296	24.00	65.28	10.72
S7	−89.59	28.75	86.40	6.129	2.375	−0.120	0.979	2.760	4.592	6.389	7.770	9.115	21.36	59.46	19.18
S11	−89.85	29.00	17.90	5.683	2.205	−0.029	0.933	2.816	4.105	5.808	7.224	8.522	14.47	62.07	23.46
S12	−89.50	28.88	27.60	6.816	1.918	0.005	1.079	4.420	5.568	6.811	8.025	9.361	25.15	67.85	7.005
S15	−89.53	28.80	80.00	6.853	1.933	−0.047	1.254	4.247	5.760	6.866	7.997	9.287	24.68	66.37	8.948
S18	−89.66	28.66	97.20	6.170	1.861	0.044	1.049	3.852	4.922	6.178	7.364	8.666	15.77	72.77	11.46
S20	−89.80	28.53	505.6	6.523	2.451	−0.203	1.117	2.847	5.318	6.933	8.165	9.530	27.47	55.63	16.89
S22	−89.84	28.75	67.20	6.131	2.263	−0.074	0.983	3.065	4.602	6.304	7.666	9.033	19.91	61.88	18.21
S29	−91.50	28.81	17.90	6.029	2.238	0.028	0.961	3.192	4.407	6.013	7.558	9.018	18.84	62.79	18.37
S34	−92.20	28.73	34.00	6.828	1.802	0.061	1.129	4.603	5.696	6.769	7.922	9.312	23.49	71.23	5.280
S35	−92.48	28.51	46.40	6.229	2.143	−0.090	1.145	3.163	4.959	6.391	7.579	8.924	18.41	66.31	15.29
S37	−92.48	29.53	1.700	6.661	2.309	−0.168	1.167	3.121	5.442	6.932	8.136	9.490	27.05	58.19	14.76
S39	−92.49	29.29	9.300	4.982	2.096	0.529	0.904	2.987	3.463	4.212	6.516	8.298	11.93	43.93	44.14
S41	−92.23	29.47	1.600	6.730	2.078	−0.088	1.245	3.818	5.557	6.810	7.972	9.312	24.25	65.03	10.71
S44	−91.40	28.53	37.60	6.278	1.954	0.004	1.099	3.857	4.984	6.302	7.491	8.843	17.39	71.50	11.12
S45	−90.96	28.48	32.40	6.293	2.050	−0.0005	0.944	3.693	4.782	6.377	7.664	9.060	19.83	66.62	13.56
S46	−90.46	28.47	39.80	6.351	2.236	0.007	0.982	3.468	4.759	6.342	7.839	9.326	22.54	62.95	14.51
S50	−89.40	28.88	28.40	6.622	2.271	−0.130	1.094	3.239	5.253	6.810	8.094	9.417	26.28	59.53	14.19
S54	−89.47	28.90	7.800	6.186	2.072	0.187	0.925	3.828	4.646	5.915	7.654	9.125	20.34	67.81	11.85
S60	−89.47	28.86	28.90	6.419	2.106	−0.021	0.946	3.715	4.952	6.513	7.874	9.208	22.79	63.89	13.32
S64	−89.41	28.82	66.70	6.438	2.503	−0.154	0.928	2.792	4.784	6.763	8.217	9.549	28.15	53.61	18.24
S68	−89.23	28.89	70.00	6.510	2.126	−0.077	1.067	3.630	5.162	6.635	7.893	9.207	23.01	64.22	12.77
AB5	−89.93	29.09	17.80	6.351	1.978	0.117	1.039	4.017	4.970	6.243	7.620	9.089	21.22	69.18	9.596
10B	−90.55	28.62	19.30	4.993	2.559	0.502	0.745	2.486	2.943	4.109	7.237	9.052	19.20	33.29	47.51
08C	−91.97	28.99	17.30	5.935	2.380	0.099	0.829	3.108	4.020	5.885	7.691	9.254	22.50	53.15	24.35
												SD	4.011	8.564	9.759

Station information: station ID, longitude, latitude, and depth. Grain size measurements (*Phi*): mean, standard deviation, skewness, kurtosis, D10, D25, D50, D75, D90, percent clay, percent silt, and percent sand. Standard deviations for percent clay, silt, and sand were calculated and are shown at the bottom of the last three columns

SD standard deviation, *Skew* skewness, *Kurt* kurtosis

2011. To keep measurement and calculations consistent, the same conservative calculation was applied to 2012 VSS samples. Our results in Section 4.3 show consistent patterns in both 2011 and 2012.

3.4 Shear stress modeling data analyses

Our erodibility measurements were conducted in multiple stations, but their spatial coverage is rather limited. Seven levels of applied shear stresses in erodibility experiments need to be compared with shear stresses on the Louisiana shelf. Based on numerical model estimates of wave and circulation patterns, Dalyander et al. (2012) from the U.S. Geological Survey developed a map of median bottom shear stress during May 2010–May 2011 for the entire nGOM. Their data were downloaded and interpolated to stations AB5, 10B, and 08C

for our study. In addition, Xu et al. (2011) developed a 3-D coupled hydrodynamics-sediment transport model for the Louisiana shelf using a Regional Ocean Modeling System, and their modeled wave-current combined shear stress in the year 1993 was interpolated to station 10B for comparison.

4 Results

4.1 Grain size

4.1.1 Spatial variation

The spatial variation in grain sizes of surficial sediment (0–1 cm) was assessed using samples collected in early

Fig. 3 Time series subplot of volume percent distribution of grain size for surficial sediment (top 1 cm) samples collected at stations AB5 (**a**), 10B (**b**), 08C (**c**), and Atch (**d**) over a 2-year period. *Solid vertical lines* distinguish the sediment size classes (*sand, silt, and clay*)
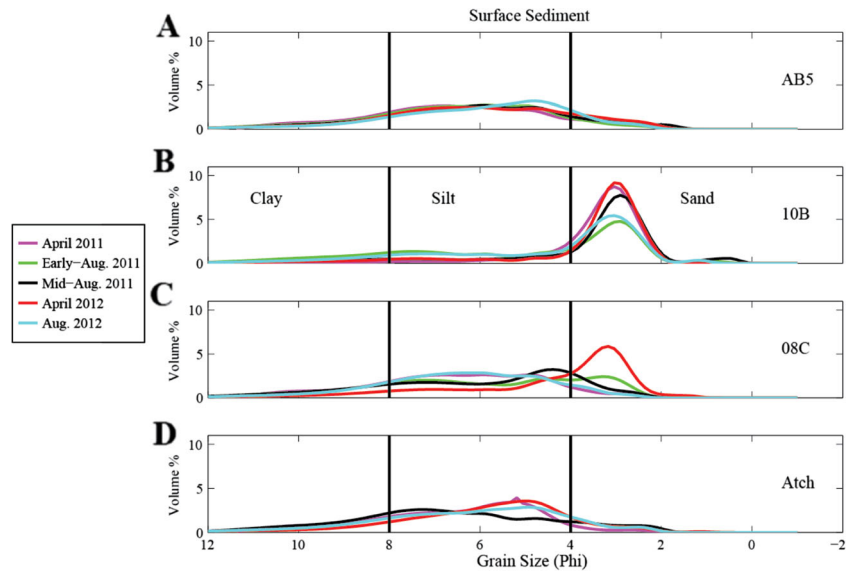
August 2011 as part of the NSF RAPID cruise. Twenty-seven stations (Fig. 1) were visited to retrieve sediment core samples for grain size analysis. The majority of sediment particles can be classified as sands (coarser than 4 Phi or 63 μm), silts (4–8 Phi or 63–4 μm), or clay size (finer than 8 Phi or 4 μm). Here, Phi scale is defined as Phi=−log2 (grain diameter in mm) according to the Udden-Wentworth classification (Brown and McLachlan 1990). The average surface sediment grain size across the entire sampling area is 6.3 Phi (12.6 μm), which corresponds to the silt size class. As shown in Fig. 2, most of the surface sediments are comprised of mostly silts. The exceptions are stations 10B (south of Terrebonne Bay, east of Ship Shoal) and S39 (west of Trinity Shoal) that are composed of

almost 50 % sands (Fig. 2a and Table 2). All other stations sampled across the nGOM show similar percentages of different grain size and are predominately composed of silty sediments (Fig. 2 and Table 2). The standard deviations (in Phi) range from 1.8 to 2.6 Phi and indicate that all the samples collected across the nGOM are either moderately sorted (1.62–2 Phi) or poorly sorted (2–4 Phi), the latter of which is more dominant among the samples (Table 2). Over half of the stations sampled were negatively skewed (−0.2 to 0 Phi) towards coarser sediment sizes, most occurring near or south of the Mississippi delta (Table 2). In addition, stations sampled have a relatively wide range of kurtosis values, most of which fall within the mesokurtic range (2.55–3.7) that indicates a wide

Fig. 4 Contour plot of down core sediment grain size percent volume for each subsample at station AB5. *Solid black lines* indicate changes in sediment size classes (*sand, silt, and clay*). The region within the *black lines* encompasses the silts
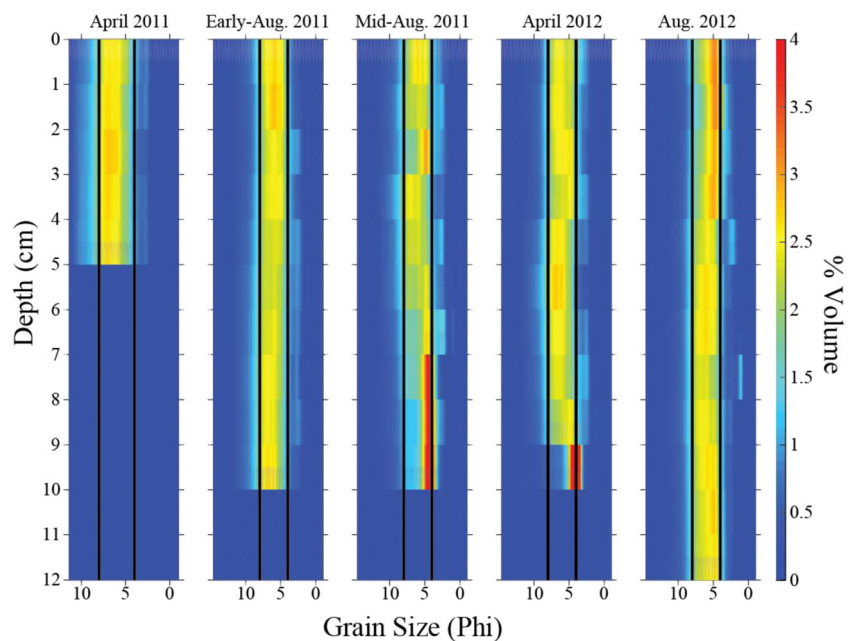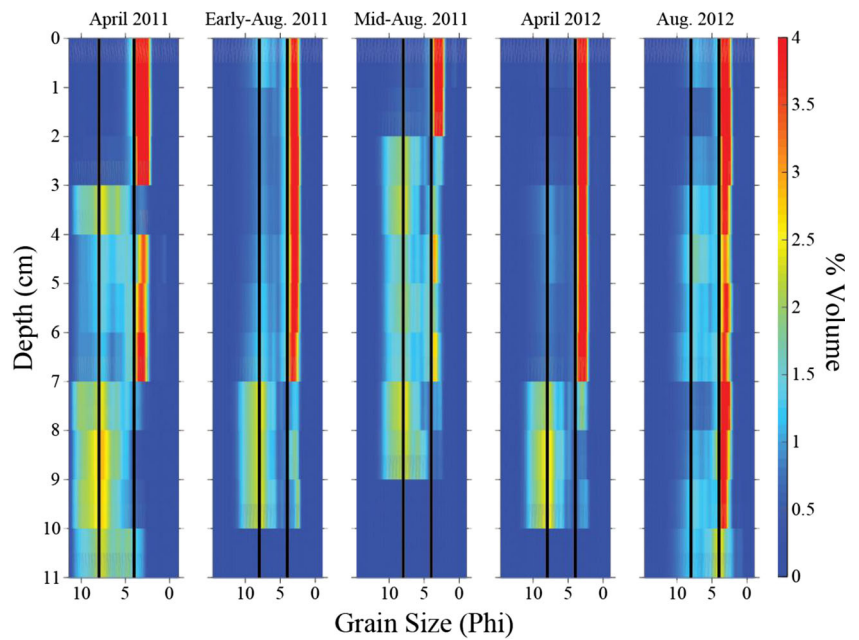
Fig. 5 Contour plot of down core sediment grain size percent volume for each subsample at station 10B. *Solid black lines* indicate changes in sediment size classes (*sand, silt, and clay*). The region within the *black lines* encompasses the silts


distribution with no distinct peaks. The rest of the samples, except for 10B and 08C which are platykurtic (1.7–2.55), increase to the leptokurtic range (3.7–7.4) (Table 2). Of the 27 stations sampled, 22 had D50 values above 6 Phi, stations 10B and S39 had D50 values of 4.2 and 4.1 Phi, respectively, and stations S11, S54, and 08C had D50 values were between 5.8 and 6 Phi (Table 2). Table 2 also includes values for D10, D25, D75, and D90 for all sampled stations. Overall, there is relatively small variability in the percentage of each grain size class among the stations sampled in this study (<10 % standard deviation for each class; Table 2), except

for two stations mentioned above that lie near Trinity Shoal and Ship Shoal, respectively.

4.1.2 Temporal variation

Temporal variation was studied at four stations over 2 years during five cruises in April 2011, early August 2011, mid-August 2011, April 2012, and August 2012: AB5, 10B, 08C, and Atch, with the exception of the early August 2011 cruise, which did not visit the station Atch. Two-year time series grain size distributions were plotted for surficial sediments (0–1 cm)

Fig. 6 Contour plot of down core sediment grain size percent volume for each subsample at station 08C. *Solid black lines* indicate changes in sediment size classes (*sand, silt, and clay*). The region within the *black lines* encompasses the silts
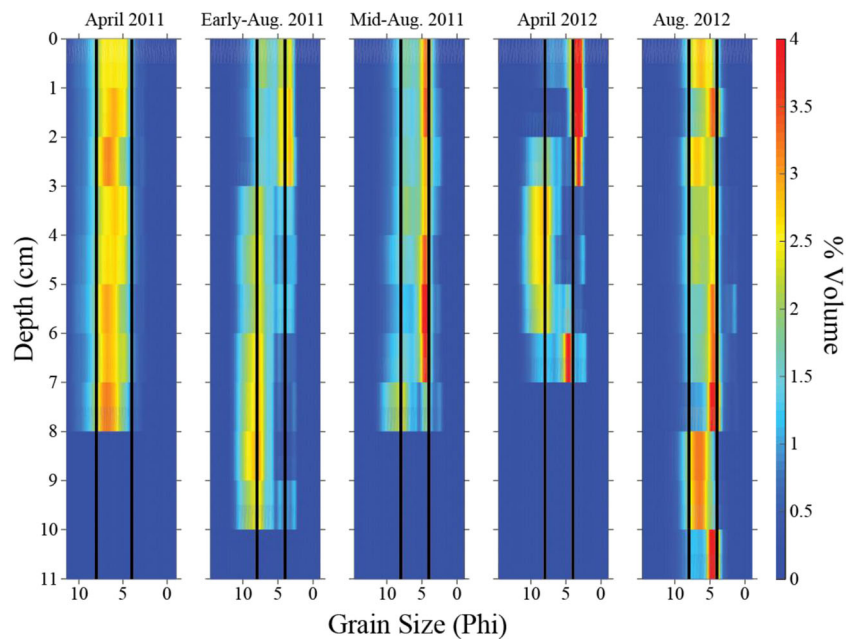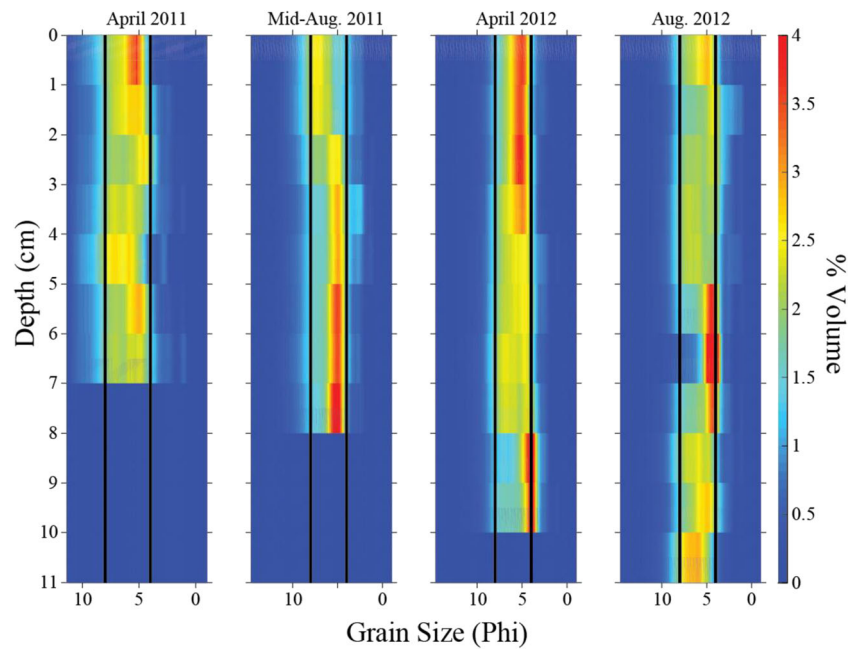
Fig. 7 Contour plot of down core sediment grain size percent volume for each subsample at station Atch. *Solid black lines* indicate changes in sediment size classes (*sand, silt,* and *clay*). The region within the *black lines* encompasses the silts

(Fig. 3) and for down core samples (Figs. 4, 5, 6, and 7) from each of the four stations. The surficial sediment distributions at stations AB5, 10B, and Atch did not vary much over the 2-year sampling period (Fig. 3). The surficial sediment distribution at station 08C does change over the 2-year period from silty material in April and August 2011 to sandier material in April 2012 then back to silty material in August 2012.

The volumetric percentage of sediment grain size is plotted as a function of depth down core for each sampling site from Figs. 4, 5, 6, and Fig. 7. The warmer colors (red and orange) indicate layers of the cores that have a higher percentage of a particular grain size range. Higher percentage volumes of grain sizes at station AB5 are present towards the bottom of the cores collected during mid-August 2011 and April 2012. The most common gain sizes are the silts as represented by the yellowish colors throughout the cores (Fig. 4). Silts are denoted as the region bounded by the black lines in Figs. 4, 5, 6, and 7. The median grain size for most of the sediment obtained at station 10B falls within the range of sandy material (Fig. 5) due to the high abundance of sand nearly throughout all cores. The sediments at station 10B also seem to be well sorted, especially surficial ones (Fig. 3) indicated by a higher volume percentage, as compared to the other stations. Mostly silty material was observed at station 08C for all of the cruises except the April 2012 cruise (Fig. 6). The upper 2 cm of the core from the April 2012 cruise was composed of sandier material relative to the other cruise samples, indicated by a higher percentage volume greater than 4 Phi (Fig. 6). All other depth intervals follow a similar pattern of silty material down core for each cruise. At Station Atch, the median grain size observed for different layers falls mostly within the range of silty material (Fig. 7).

4.2 Erodibility

Erodibility profiles were constructed for three stations (AB5, 10B, and 08C) using turbidity and TSS data (Fig. 8). These profiles indicated that greater sediment erosion at the three stations occurs when shear stress values exceed 0.3 to 0.4 Pa depending on location. The mean of the eroded masses extracted from the erodibility profiles at the 0.4-Pa shear stress is plotted in Fig. 9 to enable comparison between the April (spring) and August (summer) results from each station. This comparison in Fig. 9 shows higher mean eroded mass values during April (spring) by about 0.4 kg/m² compared to that of August (summer) sampling period at stations AB5 and 08C. However, station 10B has similar means of eroded mass during both sampling periods (Fig. 9). Examples of turbidity and rotational rate during erodibility experiments can also be seen in Fig. 10.

4.3 Volatile suspended solid

Volatile suspended solid analyses were conducted on samples collected during the April 2011, April 2012, and August 2012 cruises. The highest VSS concentrations (mg/L) were found during the application of the 0.01- and 0.6-Pa shear stresses at all three stations, making the distinct "U"-shaped pattern in Fig. 11a–c. As shown in Fig. 10, all stations exhibited higher turbidity at the lowest shear stress compared to the 0.05- and 0.1-Pa levels, which suggests the resuspension of a fluff layer from the sediment–water interface. Comparing all the stations in Fig. 11a–c, the highest VSS concentrations were observed in August 2012 for stations AB5 (120.6 mg/L) and 10B (46.4 mg/L) at the lowest shear stress level applied

Fig. 8 Erodibility profiles for each erodibility experiment over the study period for stations AB5 (**a**), 10B (**b**), and 08C (**c**) based on methods provided by Sanford and Maa (2001) and Dickhudt et al. (2009)
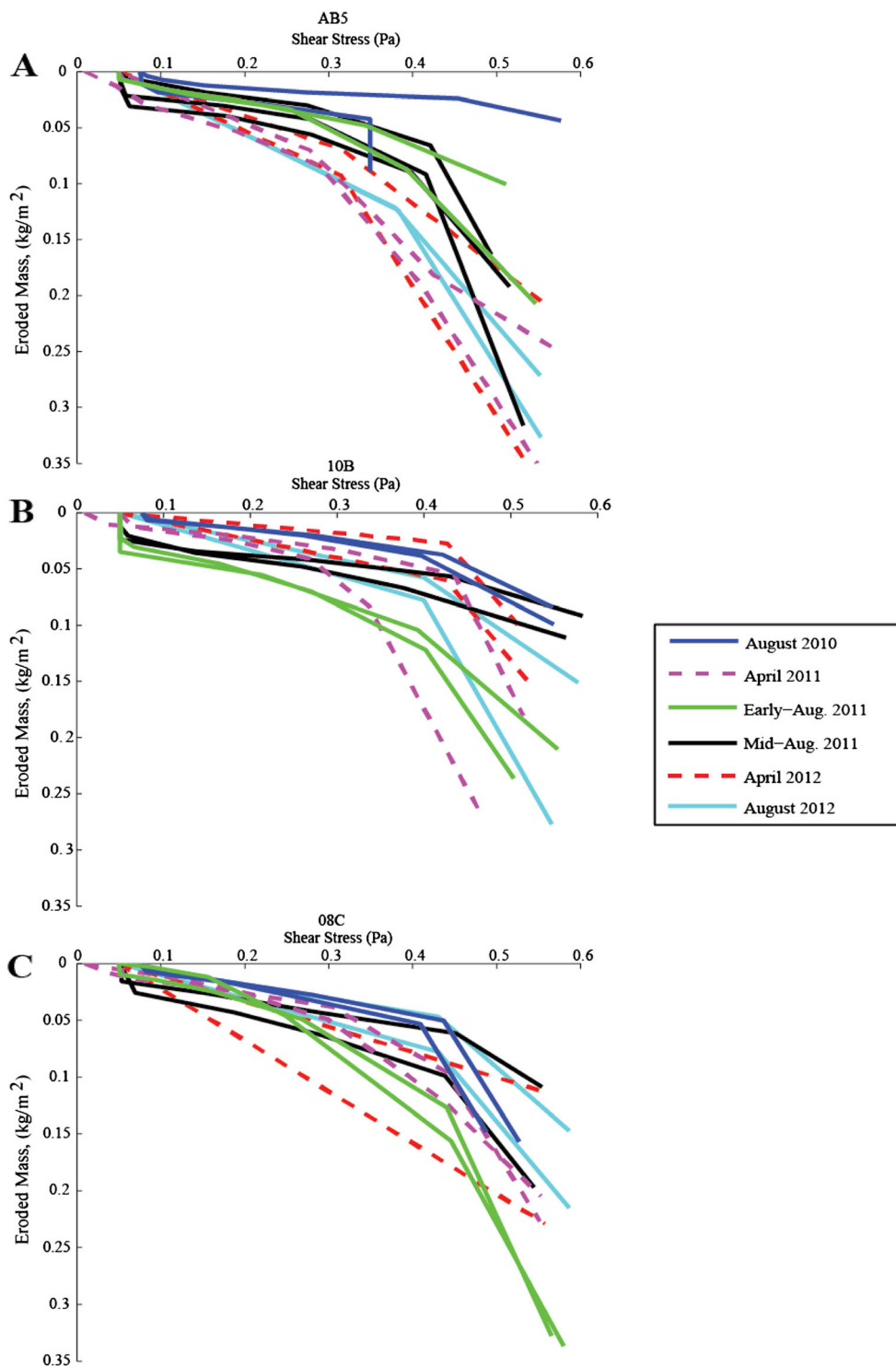

(0.01 Pa); station 08C had VSS concentrations in August 2012 of 36.26 mg/L at 0.01 Pa, but a slightly higher concentration was observed in April 2012 (39.02 mg/L) at 0.6 Pa.

The highest VSS percentage values are observed during the applications of the lower shear stress levels (0.01 and 0.05 Pa) at each of the stations (Fig. 11d–f) and are observed to be almost double the values at the highest shear stress values

(0.45 and 0.6 Pa). The VSS concentrations at station AB5 during the lowest shear stress and highest shear stress are strikingly similar, but the VSS/TSS ratios are higher at the lower shear stress level as compared to the highest shear stress. This same pattern of high VSS concentrations at 0.01 and 0.60 Pa but higher VSS/TSS ratios at 0.01 Pa only was also observed at stations 10B and 08C (Fig. 11).

Fig. 9 Bar graph representing the average values (*with error bars*) of eroded mass extracted from the erodibility profiles (Fig. 8) at the 0.4-Pa shear stress in sediment cores collected during April and August seasons. For April, a total of four samples were used to calculate the mean at each station (*n*=4). For August, a total of six samples were used to calculate the mean at each station (*n*=6)
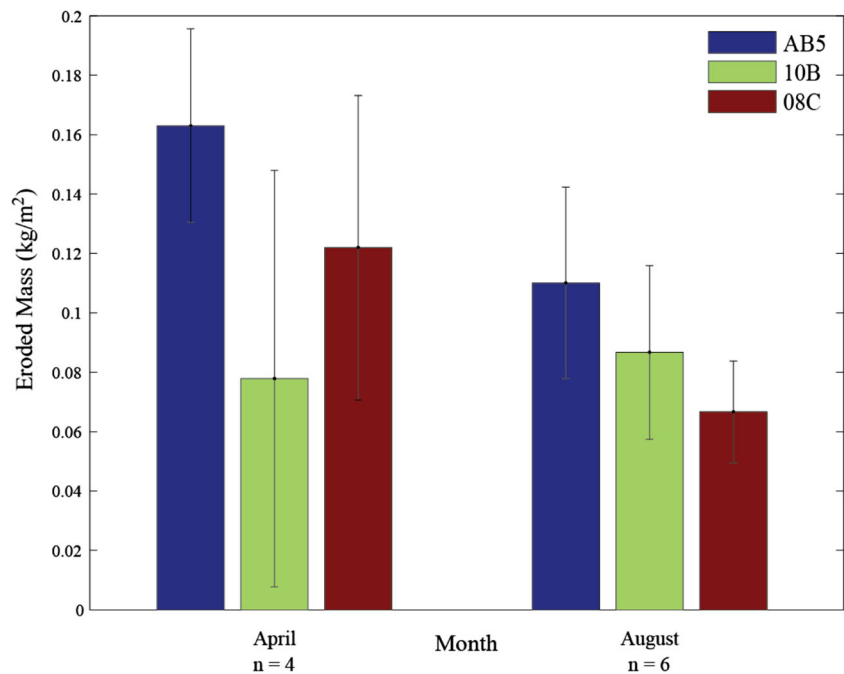
5 Discussion

5.1 Grain size

Factors affecting spatial variability of surficial sediments on the LATEX continental shelf appear to be proximity to two major river sources in the nGOM and historic delta lobe shifts. Grain size data from this study (Fig. 2) are consistent with the dominant bottom types mapped in the Gulf of Mexico Data Atlas provided by National Oceanic and Atmospheric Association (NOAA) (gulfatlas.noaa.gov), as well as with

the usSEABED database (Buczkowski et al. 2006) of percent mud for sediments in the nGOM. Each of these datasets, including the present study, illustrates those areas closer to the Mississippi and Atchafalaya River mouths are composed of a higher proportion of fine-grained sediments compared to areas on the inner shelf such as the area south of Terrebonne and Atchafalaya Bay, where sandy shoals are present (Trinity and Ship Shoals, Fig. 2). Grant et al. (1991) have suggested that the grain sizes dominating the seabed environment have important roles when it comes to carbon consumption and SOD. The variability of muddy and sandy sediments across

Fig. 10 Time series of turbidity (nephelometric turbidity units, *NTU*) and spinning rate (revolutions per minute, *RPM*) of GEMS experiments at stations AB5 (**a**), 10B (**b**), and 08C (**c**) in August 2012
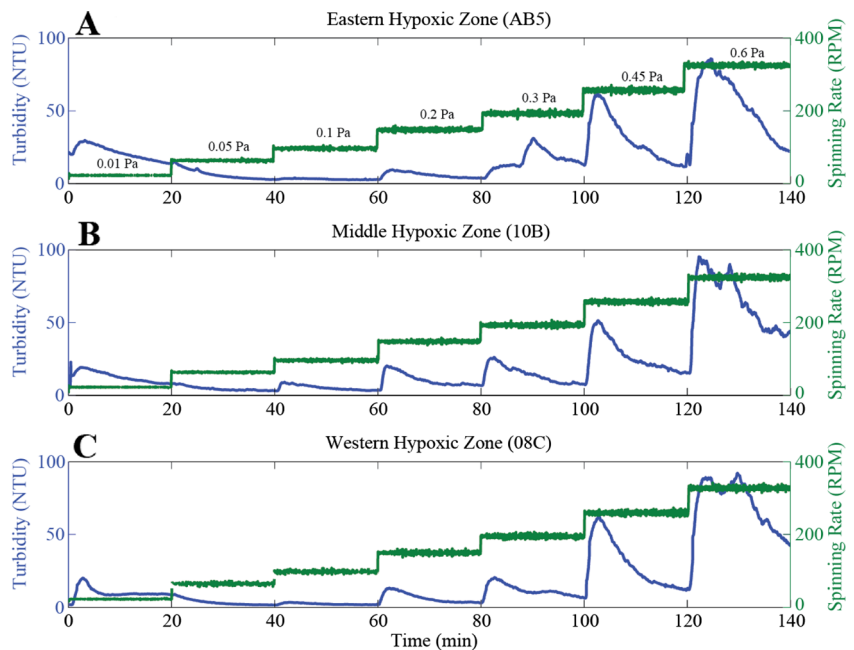
Fig. 11 Volatile suspended solid measurements from each shear stress level in milligrams per liter from samples collected and measured in April 2011, April 2012, and August 2012 at stations AB5 (**a**), 10B (**b**), and 08C (**c**). Percentage of volatile suspended solids from the total suspended solids for all cores collected in April 2011, April 2012, and August 2012 at stations AB5 (**d**), 10B (**e**), and 08C (**f**)
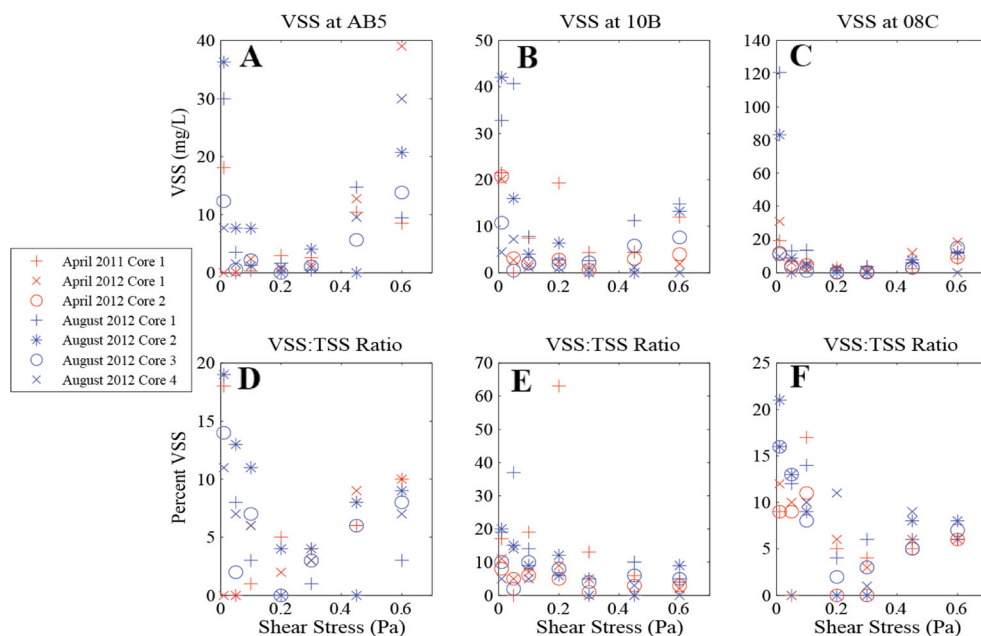
the nGOM hypoxic zone could exhibit different influences on the SOD, therefore causing spatial variability in the formation and prevalence of hypoxic waters. Newly deposited sediment materials nearer to the major river deltas are less consolidated due to the shorter residence time of those materials (Xu et al. 2014). The resuspension of these less consolidated materials along with associated organic matter that have accumulated from times of high productivity during the early spring could have major impacts on the occurrence and prevalence of hypoxic events due to the reintroduction and transport of labile material into the lower water column (Rabalais et al. 2007). The sediments across the nGOM hypoxic zone have been observed to have low levels of permeability due to fine sediment consolidation and cohesiveness; sediment porosity across this area varies with the highest value occurring nearest to the southwest pass of the Mississippi delta (Briggs et al. 2009). Thus, the spatial significance of surficial sediment grain size distribution is an important factor to consider when analyzing resuspension events that occur within hypoxic areas of the nGOM. The physical and biogeochemical inter-actions that occur between fluff material and the under-lying sediment are influenced by the properties of sed-iment that are associated with grain size such as erod-ibility, porosity, and permeability (Shepard 1989), all of which may influence bottom water hypoxia formation, prevalence, and duration, as well as SOD (Murrell and Lehrter 2010).

It has been observed that almost 95 % of the sediment load from the Mississippi River is suspended and consists of 65 % clay and about 35 % silt and fine sand particles (Johnson and Kelley 1984; Orton and Reading 1993; Coleman et al. 1998), which corresponds well with silty materials observed at

station AB5 near the mouth of the river. While our data of surficial sediment distributions show a predominantly silty composition of samples taken from across the nGOM, the volume of clay materials does not vary much among the samples taken; standard deviation of percent clay is 4.01 % (Table 2). This suggests that there is even distribution of clay materials across the entire shelf originating from the Mississippi and Atchafalaya River deltas. Data gathered from Briggs et al. (2009) indicate that sediment collected from an area with frequent hypoxia near the Mississippi delta (near station AB5) is generally comprised of poorly sorted silty clay material with a mean grain size of 8.1 Phi (4 μm). Surficial sediment samples taken from station AB5 were shown to be poorly sorted silty materials with mean grain of about 6.3 Phi (12.6 μm) (Table 2). While our dataset shows a set of values larger than those from Briggs et al. (2009) for the same area, there is an overall pattern of poorly sorted silty material observed for this area of the nGOM (Fig. 4). The presence of sandy shoals south of Atchafalaya and Terrebonne Bay is considered to be the remnant of ancient distributaries from preexisting lobes of the Mississippi River deltaic system (Coleman and Gagliano 1964). The historic lobe represents a merger of two historic deltaic systems that deposited sands since 7,000 years before present (Coleman et al. 1998). Those two sandy shoals have experienced much less hypoxia than nearby areas during the past several decades (Rabalais et al. 2007), probably due to energetic waves and currents, mobile and permeable sand, and good reoxygenation through upper water column.

Observations for percent volume of grain sizes across the LATEX shelf, with the exception of station 08C, suggest that temporally surficial sediment grain sizes remained stable at
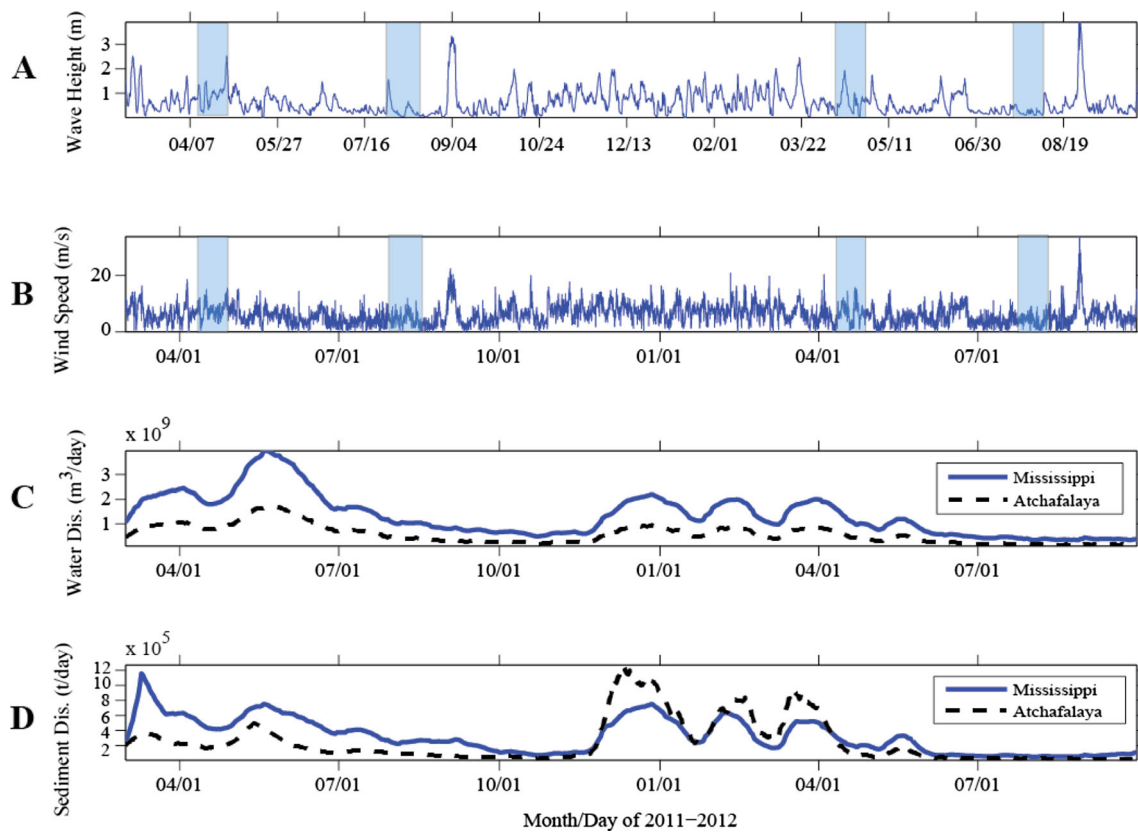
Fig. 12 a Wave height from March 2011 to September 2012 from Wavewatch III® model (provided by National Center for Environmental Prediction and National Oceanic and Atmospheric Administration) for area located at BURL1C-MAN weather station, and *shaded areas* indicated sediment sampling times. **b** Wind speed from BURL1C-MAN weather station near the Southwest Pass of the Mississippi Delta, and *shaded areas* indicated sampling times. **c** Daily water discharge of the Mississippi (at Tarbert landing) and Atchafalaya (at Simmesport) (U.S. Army Corps of Engineers, U.S. Geological Survey) Rivers. **d** Daily mean sediment discharge of the Mississippi and Atchafalaya Rivers (U.S. Geological Survey)

most stations sampled over the 2-year period (Figs. 3, 4, 5, 6, and 7). Analysis of down core distribution of sediments sizes shows that four stations have similar distribution patterns over the 2-year sampling period, which suggests either that there is not much reworking of sediment materials in the top few centimeters of the sediment surface or that newly deposited materials are similar to old ones.

Station 08C, in the western hypoxic zone, shows a shift from silty material to sandy material in the upper 2 cm of the April 2012 samples, but in August 2012, the down core profile had particle size distributions similar to those seen in the 2011 cruises (Fig. 6). This fluctuation in sediment size distribution

Table 3 Median shear stress values (Pa) for entire year (May 2010–May 2011), winter, spring, summer, and fall for stations AB5, 10B, and 08C; based on data from Dalyander et al. (2012)

Station ID	Yearly	Winter	Spring	Summer	Fall
AB5	0.0326	0.0283	0.0700	0.0259	0.0223
10B	0.0606	0.0616	0.0935	0.0361	0.0594
08C	0.0588	0.0619	0.0877	0.0433	0.0481

could have arisen from reworking of surficial sediments by increased resuspension and transport of finer grain sizes during storm events prior to April 2012 which revealed the underlying sandy sediment; however, another likely explanation is that the temporal changes reflect spatial patchiness in the sediments near the outskirts of the historic sandy shoals. The area south/southwest of Atchafalaya Bay has been observed to have exposed relict (~1,200 to 600 years before present) sediment, and therefore, sediment accumulation in this area is heterogeneous and thus accumulation rates are poorly defined (Draut et al. 2005). Also, by observing the position of sandy sediments from the usSEABED database (Buczkowski et al. 2006) in Fig. 3 of Xu et al. (2011), station 08C falls along the outskirts of this sandy area. With more analyses and sampling, the actual cause for this shift in surficial sediment composition can be better understood.
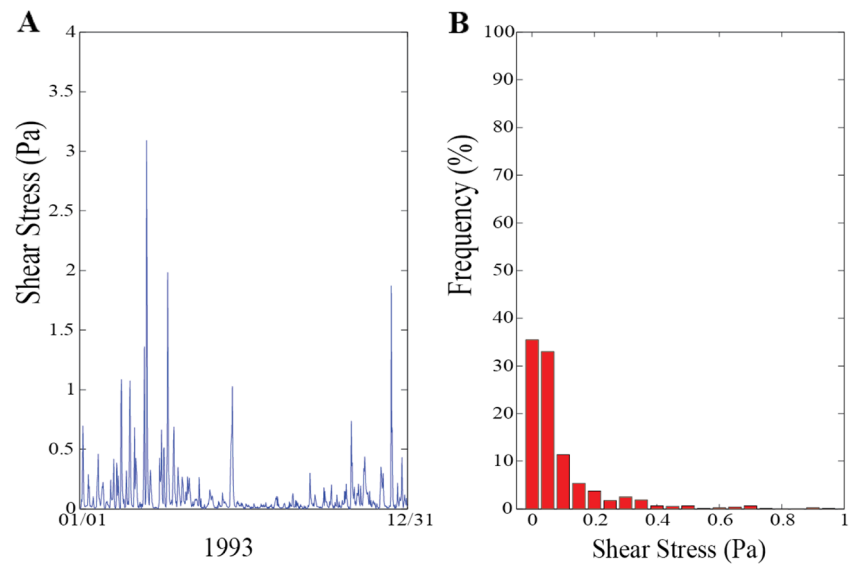
5.2 Erodibility

Temporal variability in eroded mass values at 0.4 Pa extracted from erodibility profiles at stations AB5 and 08C indicates a seasonal pattern of higher erodibility in the April cruises

Fig. 13 a Modeled hourly wind–current combined bottom shear stress (*Pa*) throughout the year 1993 at station 10B, based on data from Xu et al. (2011). **b** Occurrence frequency of modeled shear stresses in (**a**)

(spring) and lower erodibility in the August cruises (summer) (Fig. 9). However, station 10B does not show much variability by seasons which could be due to the sedimentary environment observed here, which is composed of more sand than silt/clay materials that would require higher shear stress levels for erosion. By observing the erodibility profiles at station 10B compared to AB5 and 08C, it shows that substantial erosion does not occur until shear stress reaches above 0.4 Pa. The seasonal pattern of erodibility at AB5 and 08C falls in line with the energetic wind, wave, and high river discharge patterns that occur before and during the April cruises in 2011 and 2012 (Fig. 12, shaded area), which had more occurrences of higher waves compared to August cruises. The more frequent and larger waves in April can induce a more energetic bottom boundary layer and thus increase the number of resuspension events occurring at the sediment surface. These resuspension events agitate upper seabed material and thus make the seabed more prone to erosion during lower level resuspension events that may occur later. High river discharge also brings new and relatively mobile sediment on to the seabed. The erodibility datasets from Xu et al. (2014) indicate that sediments nearer to major river deltas are less consolidated than those on the outer, central continental shelf where the majority of hypoxic events occur. The U.S. Geological survey has developed a map of median bottom shear stress during May 2010–May 2011 for the entire nGOM (Dalyander et al. 2012). Table 3 contains the median shear stress during fall (September–November), winter (December–February), spring (March–May), and summer (June–August), as well as the yearly median for stations AB5, 10B, and 08C. These modeled estimates indicate that during the summer months, seabed shear stress levels tend to be at their lowest, while during the spring months, they are highest, which corresponds well with this study's results of higher erodibility in April.

5.3 Organic matter

The high concentrations of VSS during the lowest shear stress applied (0.01 Pa) to the sediment surface are observed to be indicative of a fluff layer that is rich in OM and easily erodible (Wainright and Hopkinson 1997; Rowe et al. 2002; Dickhudt et al. 2009; Milligan and Law 2013). Our data showed the presence of a fluff layer above the sediment within these sampling areas, as indicated by the high VSS concentration in effluent samples collected during the 0.01-Pa shear stress applications as well as a higher VSS/TSS ratio (Fig. 11), which falls in line with the results of similar studies (Milligan and Law 2013; Dickhudt et al. 2009). Our VSS analysis using the GEMS system compliments the other studies that use the same methods to extract and analyze fluff material. In fact, our study is the first to use the GEMS system to help expand the knowledge of OM and fluff layer at the sediment–water interface that could influence hypoxic regimes in the nGOM.

The amounts of VSS that may be eroded from the seabed in the nGOM depends on the supply of OM to the seabed (supply, related to primary productivity), the respiration rate of OM (removal), and the sediment environment on which they are deposited (storage; high versus low sediment accumulation; sandy versus muddy environment). The VSS concentrations observed at these sample locations also appear to depend on the prevailing seasonal weather patterns, as was indicated in the August VSS measurements. During the April cruises, which occurred during times of energetic waves, lower concentrations of VSS (~20 mg/L) were observed at the lower shear stress levels overall, compared to some of the concentrations (≥30 mg/L) observed for August cruises (Fig. 11). This is expected during the spring months due to the increased wave/current energy at the bottom boundary layer which will decrease the residence time (time from

deposition to resuspension) of finer, less dense OM within the water column. In summer, more deposition of detrital material and fine particulate OM increases the OM concentration of the fluff layer present above the sediment surface, which was observed as the higher VSS concentrations ($\geq$30 mg/L). With the aid of 3-D sediment transport models, Xu et al. (2011) developed a time series of bottom shear stress levels for station 10B for the year 1993; this time series is presented in Fig. 13a along with a frequency of occurrence of various stress levels in Fig. 13b. During the model year 1993, more than 90 % of time, the simulated near-bed wave-current combined shear stress levels were less than 0.2 Pa, and about 35 % of the time shear stress levels were less than 0.02 Pa which is also comparable to Dalyander et al. (2012) shear stress dataset (Table 3). Based on the results of our study and comparisons to Dalyander et al. (2012) and Xu et al. (2011) datasets, low-energy conditions prevail for most of the year, especially during the summer months when hypoxia is present, which enables the accumulation and resuspension of a fluff layer, thus allowing for the reintroduction of OM into the lower water column. As shown in other studies (Milligan and Law 2013; Christiansen et al. 2002; Vousdoukas et al. 2011; Schaaff et al. 2006), even a very low shear stress level at 0.02 Pa is high enough to resuspend the fluff layer (Fig. 10).

6 Conclusions

Examination of grain size from samples across the nGOM suggests that there is relatively small spatial variability of surficial sediment across the nGOM, except for those areas known to be associated with the sandy shoals formed due to past Mississippi River deltaic lobe shifts and sediment reworking. There does not appear to be much temporal variability of grain sizes at the four surveyed stations, except for the changes in the top few centimeters of sediment observed in April 2012 at station 08C, which is likely to be an artifact arising from spatial patchiness of areas surrounding the historic sandy lobe or a winnowing effect of storms prior to the April 2012 sampling date. Overall, the sediment at the stations appears to be stable in time and space, and the changes in top sediment observed at 08C in this study may be rectified with more sampling data in the future.

The erodibility experiments show that there appear to be seasonal and spatial patterns based on frequency and magnitude of wind and wave conditions, which influence the composition and erodibility of suspended seabed materials across the nGOM. It also appears that the varying sedimentary environments across the nGOM have a major influence on the erodibility of seabed material. Specifically, station 10B in the coarser environment is less erodible than areas nearer to the Mississippi (station AB5) and Atchafalaya delta (station 08C). Temporal variability in seabed erodibility appears to be most

associated with seasonal weather patterns occurring in the nGOM. Energetic conditions observed in the months leading up to the April sampling periods may have increased energy levels in the bottom boundary layer, which can cause the upper seabed material to be less consolidated, thereby resulting in higher erodibility in April compared to those from August. The quiescent period during several months before August sampling periods allow sediment to consolidate and dewater, leading to less erodible sediments in August. While the underlying sediments are less erodible in August (Fig. 9), the presence and accumulation of a fluff layer enriched with OM during this period could lead to increased bacterial respiration at the sediment–water interface. VSS concentrations (as a proxy of OM) during the summer period ($\geq$30 mg/L) measured at the lowest shear stress (0.01 Pa) were found to be higher than those measured at higher shear stress levels (<20 mg/L) except the highest at 0.60 Pa. The higher degree of organic enrichment in the particles eroded during the lowest shear stress suggests the presence of an organically enriched fluff layer at the sediment–water interface. Also, showing that this OM accumulates more on the sediment surface during the quiescent summer period could have impacts on the amount of oxygen consumption coming from SOD versus the lower water column. Therefore, measuring the amounts of resuspended OM and determining the lability of that material through chemical/biological oxygen demand experiments are needed to identify if this OM being reintroduced into the water column is of primary importance to oxygen dynamics leading to hypoxia. Determining how much material, organic and inorganic, that is reintroduced into the water column and the time spent in suspension will be essential to future models that incorporate sediment transport and biogeochemical processes to study hypoxic regimes. Our study showed that the fluff layer may become resuspended at fairly low shear stress levels (0.01 Pa) and contain a higher percentage (approximately 10–50 %) of OM. Greater percentage of OM in the fluff layer, higher resuspension occurrence frequency, and very sluggish oxygenation indicate that OM sitting in the fluff layer along the sediment–water interface may play a large role in SOD compared to other biological activities occurring in the sediment. Our study has provided insights into how sediment dynamics may interact with other physical processes to influence biological and chemical regimes associated with hypoxia formation.

References

Briggs K, Watkins J, Shivarudrappa S, Hartman V (2009) Effects of hypoxia on sediment properties in the northern Gulf of Mexico. Naval Research Laboratory Public Records

Brown AC, McLachlan A (1990) Ecology of sandy shores. Elsevier Science Publishing Company, Inc., New York, p 328

Buczkowski BJ, Reid JA, Jenkins CJ, Reid JM, Williams SJ, Flocks JG (2006) usSEABED: Gulf of Mexico and Caribbean (Puerto Rico and U.S. Virgin Islands) offshore surficial sediment data release: U.S. Geological Survey Data Series 146, version 1.0.

Christainsen C, Edelvang K, Emeis K, Graf G, Jahmlich S, Kozuch J, Laima M, Leipe T, Loffler A, Lund-Hansen LC, Miltner A, Pazdro K, Pempkowiak J, Shimmield G, Shimmield T, Voss M, Witt G (2002) Material transport from the nearshore to the basinal environment in the southern Baltic Sea I. Processes and mass estimates. J Mar Syst 35:133–150

Coleman JM, Gagliano SM (1964) Cyclic sedimentation in the Mississippi River deltaic plain. Trans—Gulf Coast Assoc Geol Soc XIV:67–80

Coleman JM, Roberts HH, Stone GW (1998) Mississippi River delta: an overview. J Coast Res 14(3):698–716

Dagg M, Sato R, Liu H, Bianchi T, Green R, Powell R (2008) Microbial food web contributions to bottom water hypoxia in the Northern Gulf of Mexico. Cont Shelf Res 28:1127–1137

Dalyander PS, Butman, Bradford, Sherwood CR, Signell RP (2012) Documentation of the U.S. Geological survey sea floor stress and sediment mobility database: U.S. Geological survey open file report 2012–1137. http://pubs.usgs.gov/of/2012/1137

Dickhudt PJ, Friedrichs CT, Schaffner LC, Sanford LP (2009) Spatial and temporal variation in cohesive sediment erodibility in the York River estuary, eastern USA: a biologically influenced equilibrium modified by seasonal deposition. Mar Geol 267:128–140

Draut AE, Kineke GC, Velasco DW, Allison MA, Prime RJ (2005) Influence of the Atchafalaya river on recent evolution of the chenier-plain inner continental shelf, northern Gulf of Mexico. Cont Shelf Res 25:91–112

Emeis K, Christainsen C, Edelvang K, Jahmlich S, Kozuch J, Laima M, Leipe T, Loffler A, Lund-Hansen LC, Miltner A, Pazdro K, Pempkowiak J, Pollehne F, Shimmield T, Voss M, Witt G (2002) Material transport from the near shore to the basinal environment in the southern Baltic Sea II: synthesis of data on origin and properties of material. J Mar Syst 35:151–168

Environmental Protection Agency. http://water.epa.gov/type/watersheds/named/msbasin/marb.cfm. Accessed 8 Oct 2014

Gardner WS, McCarthy MJ, Carini SA, Souza AC, Lijun H, McNeal KS, Puckett MK, Pennington J (2009) Collection of intact sediment cores with overlying water to study nitrogen- and oxygen-dynamics in regions with seasonal hypoxia. Cont Shelf Res 29:2207–2213

Grant J, Emerson CW, Hargrave BT, Shortle JL (1991) Benthic oxygen consumption on continental shelves off Eastern Canada. Cont Shelf Res 11:1083–1097

Gust G, Muller V (1997) Interfacial hydrodynamics and entrainment functions of currently used erosion devices. Cohesive Sediments 149–174

Johnson AG, Kelley JT (1984) Temporal, spatial, and textural variation in mineralogy of Mississippi river suspended sediment. J Sediment Petrol 54(1):0067–0072

Lo EL, Bentley SJ, Xu K (2014) Experimental study of cohesive sediment consolidation and resuspension identifies approaches for coastal restoration: Lake Lery, Louisiana. Geo-Mar Lett. doi:10.1007/s00367-014-0381-3

Maa JPY, Sanford L, Halka JP (1998) Sediment resuspension characteristics in Baltimore Harbor, Maryland. Mar Geol 146:137–145

McKee BA, Aller RC, Allison MA, Bianchi TS, Kineke GC (2004) Transport and transformation of dissolved and particulate materials on continental shelf margins influenced by major rivers: benthic boundary layer and seabed processes. Cont Shelf Res 24:899–926

Meade RH, Moody JA (2010) Causes for the decline of suspended-sediment discharge in the Mississippi river system, 1940–2007. Hydrol Process 24:35–49

Milligan TG, Law BA (2013) Contaminants at the sediment-water interface: implications for environmental impact assessment and effects monitoring. Environ Sci Technol 47:5828–5834

Murrell MC, Lehrter JC (2010) Sediment and lower water column oxygen consumption in the seasonally hypoxic region of the Louisiana continental shelf. Estuar Coasts 34(5):912–924

NOAA. Gulf of Mexico Data Atlas. http://gulfatlas.noaa.gov/. Accessed 26 June 2013

Orton GJ, Reading HG (1993) Variability of deltaic processes in terms of sediment supply, with particular emphasis on grain size. Sedimentol 40:475–512

Quinones-Rivera ZJ, Wissel B, Justic D, Fry B (2007) Partitioning oxygen sources and sinks in a stratified, eutrophic coastal ecosystem using stable oxygen isotopes. Mar Ecol Prog Ser 342:69–83

Rabalais NN, Turner RE, Sen Gupta BK, Boesch DF, Chapman P, Murrell MC (2007) Characterization and long-term trends of hypoxia in the Northern Gulf of Mexico: does the science support the plan to reduce, mitigate, and control hypoxia? Estuar Coasts 30(5):753–772

Rowe GT, Cruz Kaegi ME, Morse JW, Boland GS, Escobar Briones EG (2002) Sediment community metabolism associated with continental shelf hypoxia, Northern Gulf of Mexico. Estuar 25:1097–1106

Sanford LP, Maa JPY (2001) A unified erosion formulation for fine sediments. Mar Geol 179:9–23

Schaaff E, Grenz C, Pinazo C, Lansard B (2006) Field and laboratory measurements of sediment erodibility: a comparison. J Sea Res 55:30–42

Shepard RG (1989) Correlations of permeability and grain size. Groundw 27:663–668

Turner RE, Rabalais NN, Justic D (2006) Predicting summer hypoxia in the Northern Gulf of Mexico: riverine N, P, and Si loading. Mar Pollut Bull 52(2):139–148

Turner RE, Rabalais NN, Justic D (2008) Gulf of Mexico hypoxia: alternate states and a legacy. Environ Sci Technol 42:2323–2327

United States Army Corps of Engineers. http://www2.mvn.usace.army.mil/cgi-bin/wcmanual.pl?01100 (Mississippi water discharge). Accessed 8 Oct 2014

United States Geological Survey. http://waterdata.usgs.gov/la/nwis/inventory/?site_no=07295100&agency_cd=USGS&amp (Mississippi sediment discharge). Accessed 8 October 2014; http://waterdata.usgs.gov/la/nwis/nwisman/?site_no=07381490&agency_cd=USGS (Atchafalaya water and sediment discharge). Accessed 8 Oct 2014

Vousdoukas MI, Verney R, Dufois F, Pinazo C, Sauzade D, Meule S, Cann P, Plomaritis TA (2011) Sediment dynamics in the Bay of Marseille, Gulf of Lions (France): hydrodynamic forcing vs. bed erodibility. J Coast Res 27(5):942–958

Wainright SC, Hopkinson CS Jr (1997) Effects of sediment resuspension on organic matter processing in coastal environments: a simulation model. J Mar Syst 11:353–368

Xu K, Harris CK, Hetland RD, Kaihatu JM (2011) Dispersal of Mississippi and Atchafalaya sediment on the Texas-Louisiana shelf: model estimates for the year 1993. Cont Shelf Res 31:1558–1575

Xu KH, Corbett DR, Walsh JP, Young D, Briggs KB, Cartwright GM, Friedrichs CT, Harris CK, Mickey RC, Mitra S (2014) Seabed erodibility variations on the Louisiana continental shelf before and after the 2011 Mississippi River flood. Estuar Coast Shelf Sci. doi:10.1016/j.ecss.2014.09.002